RESEARCH WORK

1. Title

Investigating a Novel Therapeutic Composition for Dry Eye Syndrome Management: *In Vitro* and *In Vivo* Studies

2. Introduction

Clinically, dry eye syndrome (DES) is characterized by reduced tear volume, quicker tear film breakup, and increased evaporation of tears from the ocular surface [1]. Extending beyond the older demographic, DES is very common in adults, with prevalence rates up to 50 % [2]. The primary approach to the management of DES involves using over-the-counter artificial tears and ocular lubricants; however, their frequent application throughout the day can pose inconvenience for patients [3]. Moreover, the prevalent multi-dose drug products available for DES management often contain preservatives. Prolonged use of these preservatives in eye drops has been linked to potential damage to the cornea and conjunctiva, causing apprehensions regarding their long-term usage [4]. Ocular inserts represent a promising therapeutic option, offering a valuable alternative for sustained drug delivery. They ensure precise dosing, provide preservative-free treatment, offer ease of administration, reduce the frequency of application, and ultimately enhance patient compliance [5]. Hot-melt extrusion (HME) offers a solvent-free, scalable, and versatile alternative to solvent-cast methods for fabricating ocular inserts, addressing issues of safety, scalability, and batch variation associated with solvent-based techniques [6]. Subsequent to the extrusion phase, the implementation of the CaliCut^{TM} system ensures an unparalleled level of precision in both calibrating polymeric strands and the precise cutting of inserts, thereby yielding well-defined dimensional control [7][8].

Significant advancements have been made in recent years in understanding the complex aetiology of DES, leading to the development of more specialised treatments. These treatments include pharmacological compounds designed at reducing inflammation, improving lipid production, and stimulating mucin and aqueous secretions from the ocular surface [9]. Developments in ocular surface treatment have highlighted the potential of castor oil as a therapeutic agent. Due to its ability to spread over the ocular surface, castor oil is anticipated to enhance tear stability, reduce tear evaporation, and minimize friction between the lid and the ocular surface. Even a small amount of castor oil has demonstrated a significant positive impact on ocular surface abnormalities [10]. In a pilot investigation conducted by Maissa et al., castor oil eyedrops exhibited a residence time of at least four hours post-instillation. This resulted in a more stable tear film and a notable decrease in ocular symptoms over the entire 4-hour follow-up period for symptomatic subjects [9]. The application of castor oil topically to the ocular surface has shown a prolonged residence time, contributing to increased tear film lipid layer thickness, improved stability, and alleviated symptoms. Recent applications of castor oil in commercial ophthalmic eyedrop preparations have proven effective in addressing tear film

lipid insufficiency and instability, showing promise in managing DES secondary to meibomian gland dysfunction (MGD), without reported side effects. Castor oil, known for its anti-inflammatory, anti-nociceptive, antioxidant, antimicrobial, and insecticidal properties, is recognized for its safety and tolerability [11]. Further, polyethylene glycol (PEG) functions as a demulcent, forming a protective layer over mucous membranes to alleviate irritation and maintain the ocular surface microenvironment [12][13]. Notably, Systane Ultra®, a commercial lubricant eye drop, incorporates PEG 400 among its ingredients, providing immediate comfort, extended ocular surface protection, and symptomatic relief for DES resulting from insufficient natural tear quantity or quality [14][15][16]. Similarly, Blink Tears®, lubricating eye drops, feature PEG 400 as an active ingredient, offering temporary relief from burning, irritation, and discomfort owing to dryness of the eye [17]. Hydroxypropyl cellulose (HPC), as found in Lacrisert®, acts to stabilize and thicken the precorneal tear film, thereby prolonging the tear film breakup time (TBUT), which is usually accelerated in patients with DES. Additionally, it functions to lubricate and protect the eye [18]. Beyond its therapeutic potential for DES, HPC possesses favourable thermoplastic properties and has been utilized in HME applications [19][20]. Furthermore, PEG 400 has also been employed in HME alongside polymers, serving as a plasticizer [21]. Moreover, the core mechanism of DES is inflammation, and dexamethasone has been used as an anti-inflammatory drug in DES [22][23][24].

Hence, the aim of this study lies in the development a castor oil and dexamethasone-co-loaded ocular insert by the HME process with laser-driven CaliCut™ technology for the management of DES. By combining ingredients such as HPC, PEG, castor oil, and dexamethasone, the objective is to target different layers of the tear film and associated inflammation for effective management of DES. The study incorporates a design of experiment (DoE) approach to examine the effects of different independent variables on distinct critical quality attribute (CQA). It integrates advanced technologies like HME and CaliCut for easy manufacturing and precise dimensional control of the developed inserts. The potential of the developed formulation in managing DES is sought to be evaluated through the systematic characterization of its physicochemical properties, release profile, and *in vivo* studies.

3. Objectives

Dry eye syndrome (DES) presents a significant challenge in ophthalmic care, necessitating innovative approaches for effective management. This research article presents a multifaceted strategy to address DES through the development of ocular inserts utilizing advanced technologies such as hot-melt extrusion (HME) and the CaliCut post-extrusion system. The formulation includes key ingredients targeting different layers of the tear film and associated inflammation, including hydroxypropyl cellulose (HPC), polyethylene glycol (PEG), castor oil, and dexamethasone. The study incorporates the design of experiments (DoE) approach, integrating HME and the precise stretching and cutting technique of CaliCut for manufacturing consistency and dimensional control of the inserts. The developed insert(s) have been systematically characterized for their physicochemical properties, release profile, and *in vivo* efficacy. Preliminary results demonstrate promising potential for the developed insert in managing DES, offering preservative-free treatment, sustained drug delivery, and improved patient compliance. This study highlights the integration of advanced technologies and formulation strategies in ocular drug delivery for effective DES management.

- To formulate and optimize ocular inserts incorporating hydroxypropyl cellulose (HPC), polyethylene glycol (PEG), castor oil, and dexamethasone.
- To evaluate the physicochemical properties and drug release profiles of the ocular inserts.
- To assess the in vivo efficacy and safety of the developed ocular inserts in animal models.

4. Materials and Methods

4.1. Materials

HPC (Klucel^{TM}-HXF grade, MW 1150 kDa) was received as a gift sample from Ashland, India, and castor oil was provided as a gift sample by Croda, India. Dexamethasone was generously supplied by Cadila Pharmaceuticals Ltd., India. PEG 400 and fluorescein sodium salt were purchased from Sigma Aldrich. Anhydrous calcium chloride, anhydrous disodium hydrogen orthophosphate, potassium dihydrogen orthophosphate, potassium chloride, sodium chloride, and benzalkonium chloride were procured from Qualigens, Thermo Fisher Scientific India Pvt. Ltd., India. Acetonitrile (ACN) of high-performance liquid chromatography (HPLC) grade was sourced from Thermo Fisher Scientific, India. Throughout the investigation, ultra-pure (MilliQ) water from the Merck Millipore system was consistently used. All remaining chemicals employed in the study adhered to analytical grade standards.

4.2. Methods

4.2.1. Preparation of castor oil and dexamethasone ocular insert

The components, namely castor oil, PEG 400, dexamethasone, and HPC, were initially mixed in a mortar and pestle before being processed into HME. In the HME process, the drug, thermoplastic polymers, and other excipients are introduced into a heated barrel containing a twin rotating screw. This configuration facilitates the transfer of the drug-polymer blend to the end of the heated barrel. As the temperature rises, the polymer melts, forming a molten mass that is constantly pumped via a die connected to the end of the heated barrel [25]. Following extrusion from the HME die, the extrudate is managed by the CaliCut post-extrusion system, which utilizes a laser dimensional gauge to facilitate stretching for optimal diameter control. The extrudate's diameter is precisely measured, and the belt speed is adjusted accordingly to achieve optimum stretching. Subsequently, the extrudates undergo cutting within the CaliCut system. Enclosed within a thermal enclosure, the belt assembly ensures consistent temperatures for effective stretching post-dimensional analysis. The temperature control plays a crucial role in enhancing the smoothness of cut edges [26].

For this experiment, the physical blend of all the functional ingredients was fed into a co-rotating twin-screw extruder (Haake^{TM} Mini CTW Micro-Conical Twin Screw Compounder, Thermo Fisher Scientific) at a constant rate. The screw speed during the extrusion process was set at 50 rpm. The extrusion was carried out at a process temperature of 160 °C, and the resulting material was extruded through a 1.5 mm diameter die to form the extrudates.

4.2.2. Post-extrusion processing using CaliCut

The CaliCut post-extrusion system (Citius, Thermo Fischer Scientific) was utilized for the precise cutting of the extrudates in order to attain the desired dimensions, i.e., diameter and length. The diameter gauge positioned at the inlet of the CaliCut measures the diameter of the extrudate and accordingly controls its stretching by providing auto feedback to conveyor belt speed as the extrudate is pulled towards the cutter (The authors have not had any present or previous financial involvement, support, or engagement in research related to CaliCut or Thermo Fischer Scientific). The extent of stretching depends on the diameter of the extrudate that is coming out of the die of the HME. Therefore, it is self-evident that if the desired diameter of the insert/implant is 0.5 mm, then the die to be used in HME should be ≥ 0.5 mm so that effective stretching can be applied for precise control of the set diameter. In addition, the effective guiding and driving of the extrudate is guaranteed by freewheel rollers. Hence, the extrudates from the die were simultaneously stretched with the belt speed set by the machine as per the desired diameter and then subjected to cutting. Since different polymeric materials may behave differently during the cutting process, which can affect the surface finish of the insert/implant, CaliCut also has heating provision to control the temperature of the extrudates. The cutting device cuts the stretched polymeric extrudate by pushing the cutting blade forward through the lever to the desired length. For our ocular insert, the nominal diameter and length were set at 1.30 mm and 3.50 mm, respectively. Accordingly, the tolerance values for the minimum and maximum diameter were set at 1.27 and 1.33 mm, respectively. Similarly, the tolerance values for the minimum and maximum length of inserts were set at 3.47 mm and 3.53 mm, respectively.

It is imperative to acknowledge that the effectiveness of any manufacturing process depends on various factors, including the specific materials used, the design of the machinery, and the intended application. The CaliCut makes the manufacturing process continuous, unlike injection molding, which is a batch process. This enhances productivity enormously in a production environment. The surface finish is primarily governed by the extruder, and exploiting the heating provision of CaliCut aids in achieving smooth edges of inserts which is important from the biocompatibility (local tissue irritation) perspective. Since the screw extruder design is conical, which leads to a very high pressure and therefore ensures that the flow is regulated, the implants are very uniform and devoid of sharp edges.

4.2.3. Design of experiments (DoE)

The experimental design incorporated DoE within the framework of QbD to facilitate formulation development. The study employed a two-factor, two-level central-composite design (CCD). Two independent variables, castor oil (A, %) and PEG 400 (B, %), were chosen and examined at two different levels: level –1 (A: 3 %, B: 2.5 %) and level +1 (A: 15 %, B: 10 %). Each insert contained 0.25 % w/w dexamethasone, with HPC comprising the remaining portion of the formulation to reach 100 %. The independent factors and their corresponding design levels utilized in this study are outlined in **Table 2**. The process parameter, such as the feeding rate in HME, was kept constant, while the temperature of HME was optimized for each batch individually. The investigation focused on assessing the impact of each of these two quantitative independent factors on critical quality attributes (CQAs), such as R1, representing the release at 4 hours. Design Expert® software (StatEase Inc., version 12, Minnesota, USA) was utilized to create and analyze the experimental design, comprising 11 experiments with 3 center points. Experiments were conducted in a random order to enhance model predictability. The significance of different model terms was evaluated by conducting an analysis of variance (ANOVA) and F-statistics on the best-fitted model. Contour plots and response surfaces were studied to elucidate the impact of each independent variable on the response. Validation of the model was conducted to assess its predictive accuracy and reliability. This involved performing confirmatory experiments to compare the practically attained values with the expected values generated by the model.

4.2.4. HPLC conditions for quantification of dexamethasone

The concentration of dexamethasone was assessed through an HPLC setup utilizing the Agilent 1260 Infinity II system. Separation was achieved using an Agilent Eclipse Plus C18 column (particle size: 5 mm, dimensions: 4.6 × 250 mm). Detection was performed with a diode array detector at a wavelength of 241 nm. The mobile phase consisted of MilliQ water (A) and acetonitrile (B), employing a gradient program with specific time points and corresponding percentages of phase A (% A): 0/60, 1/60, 2/40, 4/40, 6/60, and 7/60. The flow rate was set at 1.2 mL/min, with an injection volume of 30 µl. Each sample had a run time of 7 minutes and was analyzed using OpenLab software.

4.2.5. Uniformity of weight, dimensions, and drug content

A digital vernier caliper (General Ultratech) was utilized to evaluate the dimensions of the inserts, with three inserts randomly selected from each batch for length and diameter measurements and their respective means recorded. Additionally, a weight variation test was

conducted by randomly selecting three inserts from each batch and individually weighing them using a digital balance (Mettler Toledo), with the mean weight of the prepared ocular inserts for each batch recorded. The drug content of ocular inserts was evaluated by dissolving three inserts from each batch separately in a suitable quantity of methanol, followed by filtration of the solution and analysis of the dexamethasone content using HPLC.

4.2.6. Surface pH

The pH of the inserts was determined by immersing them in 3 mL of phosphate-buffered saline (PBS) with a pH of 7.4 ± 0.1 in glass vials. From each batch, three inserts were randomly chosen, and their pH levels were measured using a pH meter (Eutech pH 510, Thermo Fisher Scientific). The resulting pH values were averaged and reported as the mean pH for each batch [27][28].

4.2.7. Moisture absorption (%) and moisture loss (%)

The initial weights of three inserts from each batch were recorded. Subsequently, these inserts were placed in a desiccator with a super-saturated solution of sodium chloride for a period of 3 days to determine the moisture absorption. Simultaneously, three inserts from each batch were kept in a separate desiccator containing anhydrous calcium chloride for the same duration to assess the moisture loss. Throughout the testing period, the humidity level within the desiccator was monitored using a digital humidity meter (Traceable, Fisher Scientific). Following the testing period, the inserts were reweighed, and the % moisture absorption and % moisture loss were calculated using **Eq. (1)** and **Eq. (2),** respectively [19][29].

$$\%\ Moisture\ absorption = \frac{Final\ weight\ of\ insert\ (mg) - Initial\ weight\ of\ insert\ (mg)}{Initial\ weight\ of\ insert\ (mg)} \times 100 \ldots\ldots\ldots \textbf{(1)}$$

$$\%\ Moisture\ loss = \frac{Initial\ weight\ of\ insert\ (mg) - Final\ weight\ of\ insert\ (mg)}{Initial\ weight\ of\ insert\ (mg)} \times 100 \ldots\ldots\ldots \textbf{(2)}$$

4.2.8. Swelling index

To determine the swelling index of the prepared ocular inserts, the initial weight of each insert was recorded. Subsequently, the inserts were immersed in phosphate-buffered saline (PBS) with a pH of 7.4. At specific time intervals of up to 60 min (5, 10, 15, 30, 45, and 60 min), the inserts were removed, wiped with filter paper to remove excess surface PBS, and re-weighed. Measurements were conducted in triplicate, and the mean swelling index along with the standard deviation was reported. The swelling index was calculated using **Eq. (3).**

$$\%\ Swelling\ index = \frac{Weight\ of\ swollen\ insert\ (mg) - Initial\ weight\ of\ insert\ (mg)}{Initial\ weight\ of\ insert\ (mg)} \times 100 \ldots\ldots\ldots$$

(3)

4.2.9. Thermogravimetric analysis (TGA)

The thermal characteristics of dexamethasone, castor oil, PEG 400, HPC, a physical mixture of these components, and optimized inserts were analyzed using a Netzsch Thermal Gravimetric Analyzer (TGA 209 F3 Tarsus). Approximately 3-5 mg of each sample was utilized for analysis. The heating range spanned from 30 °C to 450 °C with a heating rate of 10 °C/min, and data acquisition and analysis were conducted using Netzsch Proteus software.

4.2.10. Differential scanning calorimetry (DSC)

DSC analysis was conducted to assess the thermal characteristics of the optimized insert, its constituent ingredients, and the physical mixture. The measurements were carried out using the DSC-60 Plus (Shimadzu). Samples, each weighing approximately 5 mg, were placed and hermetically sealed in aluminium pans. Subsequently, the samples were subjected to a scanning process within a temperature range of 30 to 300 °C, employing a consistent heating rate of 10 °C/min. Nitrogen purging was maintained throughout the analysis at a flow rate of 50 mL/min.

4.2.11. X-Ray diffraction (XRD)

XRD patterns were obtained for various samples, including the pure drug, HPC, and the physical mixture of the optimized formulation and optimized insert. The XRD analysis was performed under ambient conditions using an X-ray diffractometer (Rigaku Miniflex II) equipped with nickel filtered Cu K radiation. The operating voltage was set to 3 kV, with a current of 5 mA. Scanning was conducted at a controlled rate of 4°/min, covering a range of 5 to 40° 2θ [30][31].

4.2.12. Attenuated Total Reflectance Fourier Transform Infrared (ATR-FTIR) spectroscopy

The ATR-FTIR spectra of dexamethasone, castor oil, PEG 400, HPC, a physical mixture of these components, and optimized inserts were obtained within the scanning range of 4000–600 cm^{-1} using the Bruker ATR (Alpha opus 7.5) at ambient temperature. The ATR-FTIR study aimed to evaluate the interactions among the functional ingredients used in the development of the ocular insert.

4.2.13. Optical microscopy

The morphology of the fabricated inserts was examined using an optical microscopy (Leica ICC50 E) and FE-SEM (Zeiss Sigma 300, Germany). For the optical microscopy analysis, the samples were directly observed by placing them on a slide and examining them under the microscope. No additional sample preparation techniques were employed.

4.2.14. Scanning electron microscopy (SEM) and energy dispersive X-ray spectroscopy (EDS)

The surface morphology of samples, namely pure dexamethasone; a physical mixture comprising dexamethasone, castor oil, PEG 400, and HPC; and the optimized insert formulation, was investigated using a field emission SEM (Zeiss Sigma 300). Each sample was securely positioned on SEM stubs and affixed using double-adhesive tape. Before imaging, a thin layer of gold was sputter-coated onto the samples under an argon atmosphere, employing the Quorum (Q150R S Plus) sputter coater. Furthermore, elemental analysis using EDS was performed on the cross-sections of the optimized inserts. This analysis aimed to track the distribution of dexamethasone by identifying the presence of fluorine (F) atoms, in addition to carbon (C) and oxygen (O), within the insert [32].

4.2.15. *In vitro* release

The *in vitro* drug release from the optimized ocular insert was examined by immersing each insert in a glass beaker containing 5 mL of PBS with a pH of 7.4. A mesh was carefully positioned over the insert, and magnetic beads were placed on top of the mesh. The beaker was then subjected to controlled conditions on a multi-station hot plate (IKA RT 10) set at 100 rpm and kept at a temperature of 34 ± 0.2°C. Sampling was performed at predetermined time intervals: 30 minutes, 1 hour, 3 hours, 6 hours, 9 hours, 12 hours, and 15 hours. The collected samples were analyzed using HPLC to determine the concentration of dexamethasone. The experimental procedure was performed in triplicate, and the results are expressed as the mean ± standard deviation (SD) [21].

4.2.15.1. Determination of drug release kinetics

For gaining deeper insights into the mechanisms underlying the release of drug from polymeric matrices, the *in vitro* release data of the ocular inserts were analysed (DDSolver software). Various kinetic models, namely zero-order, first-order, Higuchi, Korsmeyer-Peppas, and Hixson-Crowell, were employed to analyse the release data. The results obtained from this analysis were assessed based on statistical parameters such as adjusted coefficient of determination (R^2), Akaike Information Criterion (AIC), and Model selection criteria (MSC).

The model exhibiting the highest correlation was selected to describe the primary release mechanism [33], [34].

4.2.16. *In vivo* irritation study

The ocular irritation potential of the developed inserts was assessed by the Draize eye irritancy test. This test evaluates the ability of the inserts to cause harm to the cornea, iris, and conjunctiva on application to the eye [22]. Prior to the test, the inserts underwent sterilization using UV radiation. The study protocol received approval from the Institutional Animal Ethics Committee of L.M. College of Pharmacy, India (LMCP/IAEC/23-01/0074). For the eye irritancy test, adult albino rabbits weighing approximately 2.5 to 3.5 kg of either sex were used. The eye irritation potential of the insert was evaluated using three rabbits as test subjects [29]. Once the lower lid was carefully pulled from the eyeball, the insert was then placed into the conjunctival sac of one eye for each rabbit. The lids were then carefully held together for a few seconds to ensure the insert remained in place. The other eye of the rabbits remained untreated and served as a control. Throughout the study, the test animals were regularly examined to observe any signs of irritation. The evaluation of eye irritation followed the guidelines set by the Organisation for Economic Co-operation and Development (OECD) Test No. 405: Acute Eye Irritation/Corrosion guidelines, which employs a grading system to assess the condition of the cornea, iris, conjunctiva, and chemosis [35] (**Table 1**).

Table 1 Assessment of eye irritation of rabbits

Aspect	Grades based on clinical observations
Cornea	0 (normal), 1 (diffuse areas of opacity), 2 (easily noticeable translucent area; slightly obscured iris details), 3 (nacrous area rendering iris details invisible), 4 (opaque cornea)
Iris	0 (normal), 1 (deepened rugae, congestion, swelling, moderate circumcorneal hyperaemia; sluggish response to light), 2 (hemorrhage; no reaction to light)
Conjunctiva	0 (normal), 1 (slight hyperemia), 2 (crimson colour), 3 (diffuse beefy red colour)
Chemosis	0 (normal), 1 (some swelling above normal), 2 (swelling accompanied by partial eversion of lids), 3 (swelling with lids about half closed), 4 (swelling with lids closed more than halfway)

4.2.17. *In vivo* efficacy study

The efficacy of the developed optimized inserts was evaluated. Adult albino New Zealand rabbits (n = 6), weighing between 2.5-3.5 kg, were utilized for the irritancy study. DES was

induced by the topical administration of 0.1% benzalkonium chloride to both eyes twice daily for 7 days. After the cessation of benzalkonium chloride administration, the right eye in each rabbit received the treatment, while the other eye served as a control.

4.2.17.1. Tear volume measurement

A Schirmer I tear test was performed by placing a Schirmer test strip (Tear Touch, Madhu Instruments Pvt. Ltd., India) along the palpebral conjunctival vesica, aligning it with the lateral one-third of the lower eyelid. The strip was held in place for a specified duration, and subsequently, the length of the wetted portion of the strip was measured in millimetres (mm). The right eye was treated with insert, while the left eye served as control. Tear volume was assessed before model induction (baseline) and on day 11 following the application of sterilized optimized inserts in right eye. Additionally, tear volume was evaluated in the untreated eye where dry eye was induced [36][37][38].

5. Statistical analysis

The analysis of the CCD was conducted using Design Expert 12.0 software, licensed by Stat-Ease Inc. (Minneapolis, USA). A one-way ANOVA (Bonferroni) was employed for all comparisons of aqueous tear secretion, utilizing GraphPad Prism 8.3.0 Software (USA). A significance level of $p < 0.05$ was employed, considering values below this threshold as statistically significant.

6. Results and discussion

6.1. Formulation development

HME represents a continuous pharmaceutical manufacturing process wherein polymeric materials are pumped using a rotating screw at temperatures exceeding their glass transition temperature (Tg) and, at times, surpassing the melting temperature (Tm). The process aims to attain molecular-level mixing of active compounds with thermoplastic binders, polymers, or both [21][39]. The CaliCut post-extrusion system stands out as a versatile and highly modular tool designed for the accurate calibration of polymer strands and the precise cutting of well-defined inserts. Its adaptability allows it to meet a wide range of product specifications with ease [26]. In our study, the fabrication process involved the successful production of inserts from all batches using a Haake Mini CTW extruder and CaliCut post-extrusion system. All functional ingredients underwent exposure to processing temperature (170°C) and shearing stresses during the HME process. The extrudate emerging from the HME die, followed by precise diameter laser gauging, underwent stretching by the CaliCut belt and was cut based on input dimensional controls. This entire process is illustrated in **Fig. 1**, accompanied by representative images of the developed inserts and their respective dimensions.

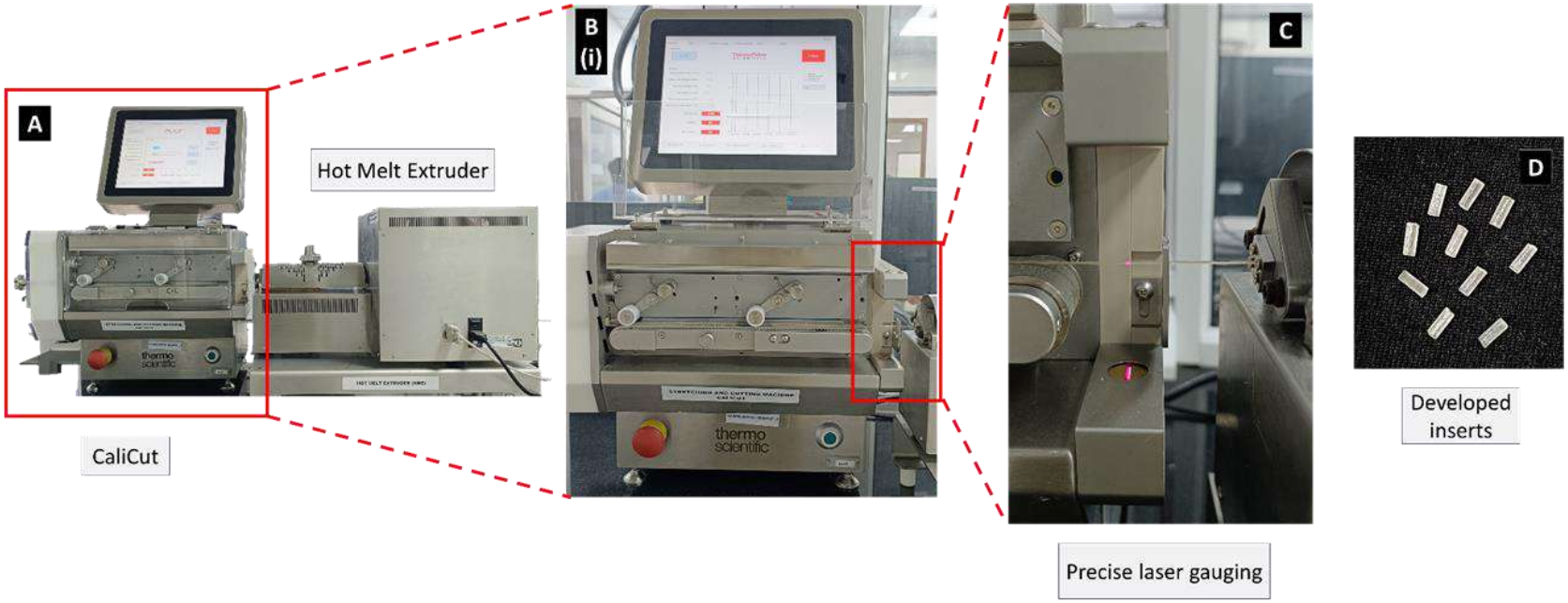
A
Hot Melt Extruder
CaliCut
B
(i)
C
Precise laser gauging
D
Developed
inserts

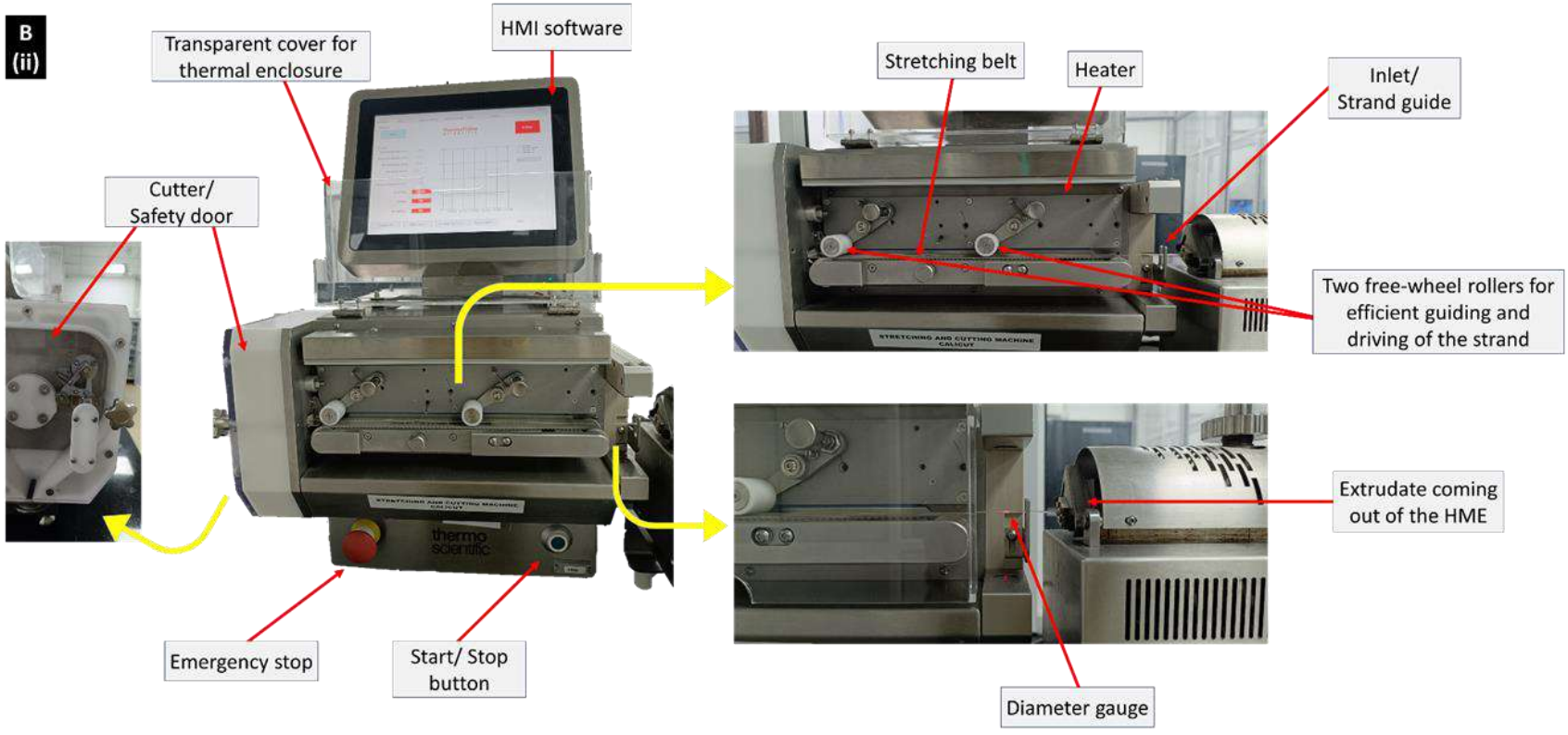
B
(ii)
Transparent cover for
thermal enclosure
HMI software
Cutter/
Safety door
Emergency stop
Start/ Stop
button
Stretching belt
Heater
Inlet/
Strand guide
Two free-wheel rollers for
efficient guiding and
driving of the strand
Extrudate coming
out of the HME
Diameter gauge

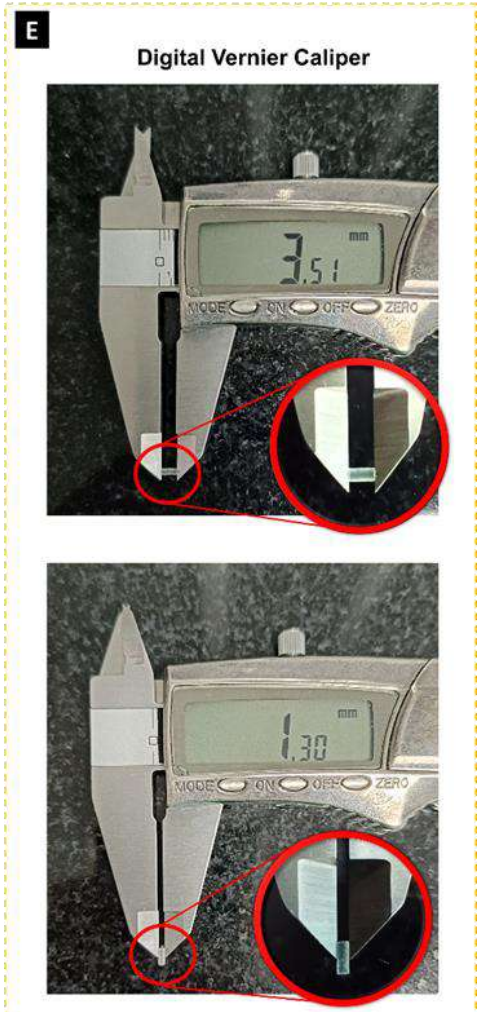
E
Digital Vernier Caliper
3.51
mm
MODE
ON
OFF
ZERO
1.30
mm
MODE
ON
OFF
ZERO
Length and diameter of the developed
insert respectively

Fig. 1. Visual representation of **(A)** Extrudate coming out of the die of HME, **(B, i)** Stretching by CaliCut with precise measurement of diameter using laser, **(B, ii)** Technological stratification of CaliCut, **(C)** Cutting of the extrudate after passing on through the belt, **(D)** Oil-loaded inserts obtained from HME and CaliCut, and **(E)** Analysed length and diameter of the developed insert.

In the case of CaliCut, the extrudate that emerges from the die of the HME (**Fig. 1A**) is constantly measured for its diameter using a line laser positioned at the machine's inlet (**Fig. 1B, 1C**). This diameter measurement assists in controlling the belt speed and facilitating the stretching of the extrudate (**Fig. 1B(ii)**). Additionally, the belt speed can be manually adjusted to meet specific requirements. During this study, to achieve the desired diameter of the inserts within specified tolerances, the system was operated in an automated mode. Laser measurements were used to guide the adjustments of the belt speed, ensuring precise control over the stretching of the extruded strand, and enabling accurate diameter adjustments. The stretched extrudate, guided by two efficient freewheel rollers, is conveyed to the cutter. The transparent cover ensures that the extrudate is thermally enclosed, maintaining its consistency for the cutting process. The software allows for configuring the temperature of the heater. For this study, the heating temperature of the stretching and cutting machine was optimized at 55 °C to achieve inserts with smooth edges. The process concludes with the collection of inserts that have been cut by the CaliCut, following their transition from the belt to the cutter. **Fig. 1(A-E**) provides a visual representation of the entire process involved in the preparation of ocular inserts, including specific details of the CaliCut process and its relevant parts.

Since CaliCut relies on laser measurements and belt speed adjustments to control the stretching and cutting of the extrudate, having well-defined dimensions (**Fig. 1E**) ensures that the inserts meet the specified tolerances. When the inserts have consistent dimensions, it allows for better control over the cutting process, resulting in uniform and accurately sized inserts. The success of the CaliCut system is contingent upon the inserts having well-defined dimensions with smooth edges and desired surface characteristics, as this directly influences the precision, quality, and performance of the ocular insert

6.2. Experimental design

In this study, DoE was utilized as a structured and systematic approach to assess how parameters influence responses within predetermined ranges [40]. The CCD was employed for formulation optimization, facilitating exploration of the impacts of independent variables in relation to dependent variables. A total of 11 experimental runs were conducted, as suggested by the DoE, and the observed responses generated by the software are presented in **Table 2**. The Two-Factor Interaction (2FI) model was selected as the best-fit model. An ANOVA test was applied to evaluate the significance of the various terms in the 2FI model and their influence on the response, as detailed in **Table 3**. The statistical analysis confirmed the significance of the regression model (p-value < 0.05) for the response. The predicted R^2 value (0.7310) closely aligned with the adjusted R^2 value (0.8767), with a difference less than 0.2, signifying model accuracy. Adequate precision, with a signal-to-noise ratio of 14.0019, surpassing the threshold of 4, confirmed a strong signal and suggested the model's effectiveness in navigating the design space. Further, the model F-value was 24.70, implying that the model was significant. P-values less than 0.0500 indicated that the terms in the model were statistically significant, validating its reliability. A Lack of Fit F-value of 8.69 suggested that the Lack of Fit was not statistically significant relative to the pure error. The 2FI model equation with coded factors for R1 as a function of the independent variable is presented in **Eq. (4).** A positive coefficient in the regression equation implies that an increase in the factor results in a higher response, whereas a negative coefficient indicates the opposite effect.

$$Release\ at\ 4\ hours\ = +62.23 + 3.33\,A + 3.39\,B - 1.29\,AB \ldots\ldots\ldots \textbf{(4)}$$

Table 2 Formulations batches and their observed responses according to the CCD design matrix

Design					
Formulation	**Factor 1**	**Factor 2**	HPC conc.	Drug conc.	**Response 1**
	A: Castor oil conc.	B: PEG conc.			R1: Release at 4 hours
	%	%	%	%	%
F1	15	2.5	82.25	0.25	64.78
F2	9	11.5	79.25	0.25	65.76
F3	15	10	74.75	0.25	68.75
F4	3	10	86.75	0.25	64.40
F5	9	0.95	89.8	0.25	55.85
F6	3	2.5	94.25	0.25	55.26
F7	9	6.25	84.5	0.25	63.52

F8	17.5	6.25	76	0.25	64.96
F9	0.51	6.25	84.5	0.25	55.90
F10	9	6.25	84.5	0.25	63.10
F11	9	6.25	92.99	0.25	62.29

Table 3 ANOVA for 2FI model: Release at 4 hours

Source	Sum of Squares	df	Mean Square	F-value	p-value	
Model	187.68	3	62.56	24.70	0.0004	significant
A-CO	88.94	1	88.94	35.12	0.0006	
B-PEG	92.05	1	92.05	36.35	0.0005	
AB	6.69	1	6.69	2.64	0.1481	
Residual	17.73	7	2.53			
Lack of Fit	16.95	5	3.39	8.69	0.1064	not significant
Pure Error	0.7798	2	0.3899			
Cor Total	205.40	10				

The contour plot provides a two-dimensional (2D) representation of the response concerning numeric factors and/or mixture components, illustrating their relationship [41], while the three-dimensional (3D) surface plot serves as a projection of this relationship, providing comprehensive visualization into the data's behaviour. Both the 2D contour plot and the 3D response surface plot for the response are graphically illustrated in **Fig. 2.** An interpretation was derived from these plots, suggesting that increasing the concentrations of castor oil results in higher drug release at 4 hours. Similarly, an increase in PEG concentrations also leads to increased drug release at 4 hours.

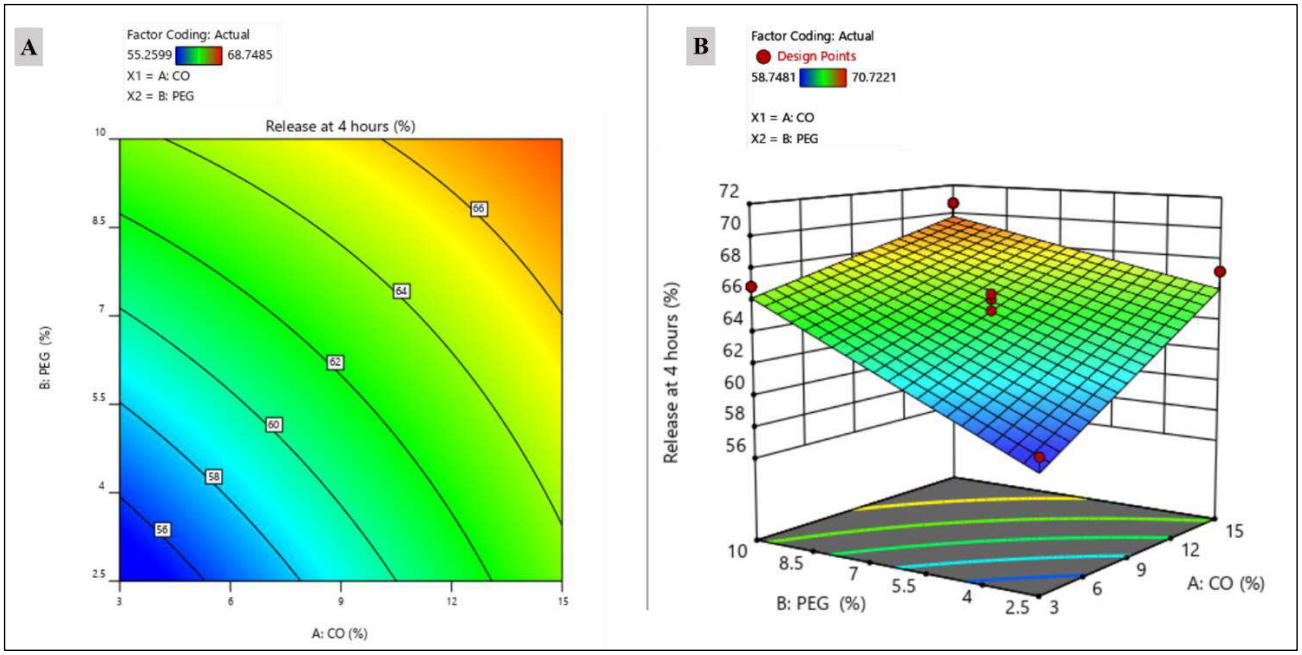

Fig. 2. (A) 2D contour plot and **(B)** 3D surface response plot illustrating the effect of independent factors on the CQA.

A multidimensional combination and interaction of specified input parameters that have been developed to ensure product quality is provided by design space [42]. Obtained by setting the response to meet a lower drug release at 4 hours (< 65 %), the yellow area observed in **Fig. 3** represents the design space on the overlay plot. Further analysis of the design revealed that increasing the concentrations of castor oil and PEG 400 led to a corresponding increase in drug release at 4 hours. Consequently, although minimum drug release was observed at lower concentrations of castor oil and PEG 400, these components are known for their functional properties and anticipated therapeutic effects in managing dry eye. Hence, to balance formulation considerations and efficacy, formula (F7) comprising 9 % castor oil, 6.25 % PEG 400, 84.5 % HPC, and 0.25 % dexamethasone was selected as the optimized formula within the design space and subjected to further *in vitro* and *in vivo* characterization. Validation of the model was conducted through confirmatory experiments, where the agreement between the practically attained values and the expected values confirmed the predictability of the model, thus validating it.

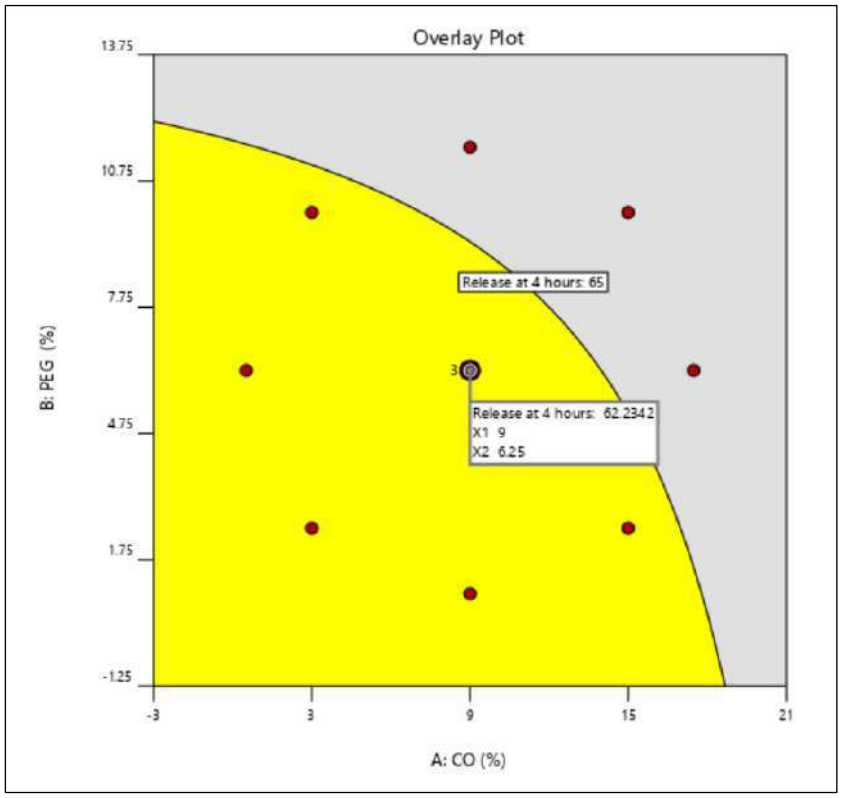

Fig. 3. Overlay plot for optimized parameters.

6.3. Uniformity of weight, dimensions, and drug content

The uniformity and consistency of ocular inserts were achieved through the application of both the HME and CaliCut techniques. The formulated ocular inserts showed a satisfactory semi-transparent appearance and uniform, smooth surfaces (**Fig. 1C**). The weight variation of the inserts was assessed to ensure consistency and uniformity within each batch. The inserts were found to have an average weight of approximately 5 mg, with dimensions of 1.30 mm (diameter) × 3.50 mm (length). The drug content ranged between 98.04 and 101.61, with SD values below 5.0 % for all runs, confirming the uniformity of drug content within the polymeric matrix due to the molecular-level mixing of functional ingredients during HME processing. The measured parameters, such as weight, diameter, length, and drug content for inserts (n = 3) from all batches, are summarized in **Table 4.**

Table 4 Weight, diameter, length, and drug content of developed ocular inserts (mean ± SD, n = 3)

Formulation	Weight (mg)	Diameter (mm)	Length (mm)	Drug content (%)	Moisture absorption (%)	Moisture loss (%)	Surface pH
F1	4.98 ± 0.09	1.31 ± 0.01	3.50 ± 0.01	100.52 ± 3.15	2.95 ± 0.76	2.37 ± 1.22	7.37 ± 0.01
F2	4.99 ± 0.09	1.31 ± 0.02	3.50 ± 0.01	100.11 ± 3.58	3.22 ± 0.52	2.10 ± 0.11	7.39 ± 0.01
F3	5.04 ± 0.06	1.29 ± 0.02	3.51 ± 0.01	101.61 ± 3.28	3.36 ± 0.77	1.30 ± 0.41	7.39 ± 0.03
F4	5.04 ± 0.07	1.31 ± 0.01	3.49 ± 0.01	99.17 ± 3.15	2.71 ± 1.66	1.55 ± 1.09	7.38 ± 0.01
F5	5.06 ± 0.04	1.31 ± 0.02	3.51 ± 0.01	98.84 ± 2.79	2.77 ± 1.13	1.75 ± 0.57	7.41 ± 0.01
F6	5.02 ± 0.04	1.31 ± 0.02	3.51 ± 0.02	98.04 ± 3.88	3.09 ± 0.69	1.44 ± 0.87	7.39 ± 0.02
F7	5.04 ± 0.06	1.31 ± 0.01	3.50 ± 0.01	100.46 ± 2.17	2.70 ± 0.53	1.64 ± 0.16	7.40 ± 0.02
F8	5.01 ± 0.06	1.31 ± 0.02	3.51 ± 0.01	99.63 ± 2.69	2.83 ± 1.18	1.74 ± 0.35	7.38 ± 0.02
F9	5.03 ± 0.13	1.30 ± 0.02	3.50 ± 0.01	98.52 ± 2.68	2.55 ± 0.58	2.01 ± 0.64	7.39 ± 0.03
F10	4.99 ± 0.09	1.31 ± 0.01	3.50 ± 0.00	99.84 ± 2.66	2.62 ± 0.39	1.53 ± 0.23	7.40 ± 0.02
F11	5.01 ± 0.10	1.31 ± 0.02	3.51 ± 0.01	99.44 ± 3.27	2.69 ± 0.52	1.55 ± 0.44	7.39 ± 0.01

6.4. Surface pH

Normal tears have a pH of about 7.4. The eye can tolerate products across a pH range from about 3.0 to about 8.6, contingent upon the buffering capacity of the formulation [43]. The surface pH of all the inserts fell within the range of 7.37–7.41, as demonstrated in **Table 4**,

making them suitable for ocular applications due to their compatibility with both the tolerable pH range of the eye and the normal human tear pH range.

6.5. Moisture absorption (%) and moisture loss (%)

The developed inserts were subjected to assessment for moisture absorption and moisture loss capacity, with findings detailed in **Table 4**. Notably, all recorded values for moisture absorption and moisture loss remained below 5 %. This observation holds significance, given that moisture uptake by the formulation can profoundly influence diverse properties, including chemical degradation rates and susceptibility to microbial contamination [19]. The moisture absorption values ranged from 2.55 ± 0.58 % to 4.83 ± 0.60 %, while moisture loss values ranged from 1.30 ± 0.41 % to 2.37 ± 1.22 % across all experimental runs. Moreover, the physical integrity of the inserts remained unchanged even under extreme humid and dry conditions.

6.6. Swelling Index

The swelling index serves as a significant measure reflecting the bioadhesive properties of polymeric inserts and demonstrates their water-retaining capacity [27]. The adherence of the dosage form to the biological surface initiates once the polymer begins to swell, and this adherence strengthens with the increasing hydration level of the polymer. By quantifying the degree to which the polymer swells upon exposure to water, the swelling index provides insights into its ability to adhere effectively to biological surfaces. HPC, being a hydrophilic and swellable polymer with a high molecular weight, facilitated increased hydration [19]. With time, the water absorption and swelling of the polymer increased, a trend that can be attributed to the polymer's hydrophilicity. The swelling index of the optimized insert was assessed for a duration of 60 minutes, as depicted in **Fig. 4.** Furthermore, upon hydration, the inserts tend to swell, allowing them to readily conform to the contour of the eye, thus facilitating conveniency.

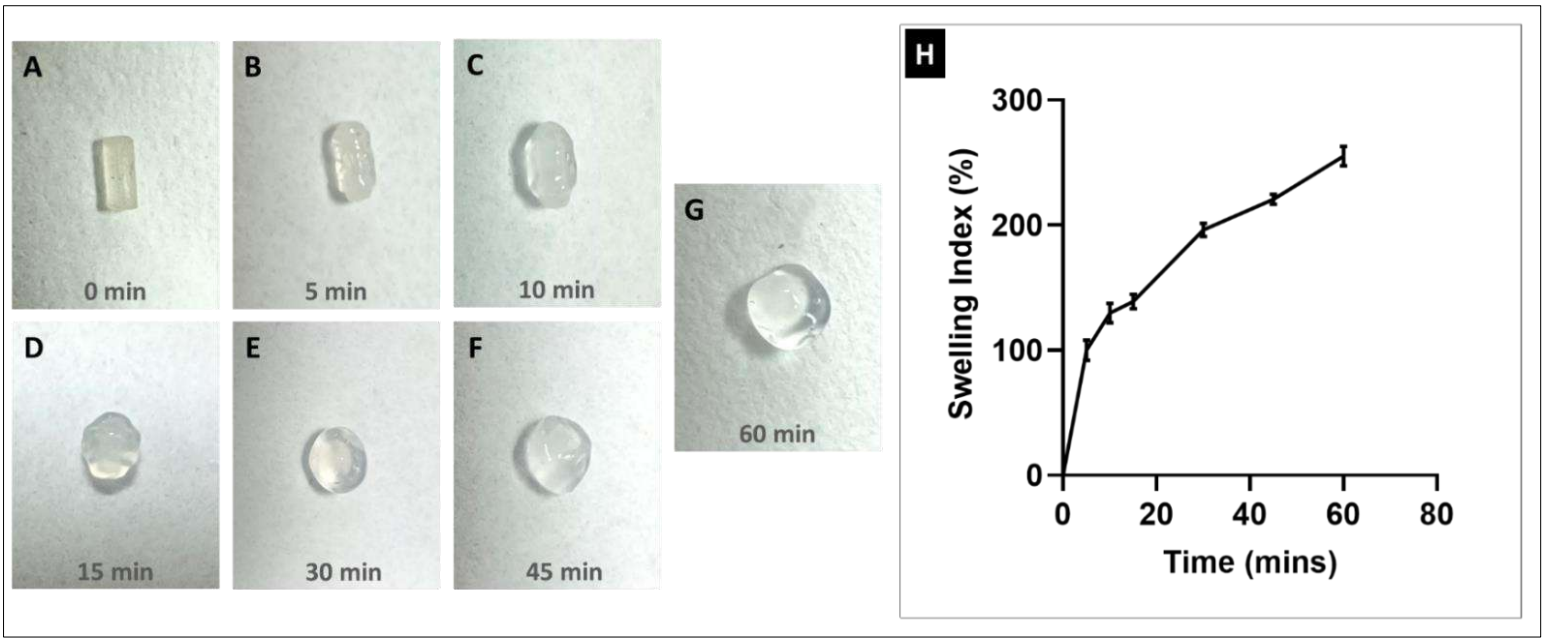

Fig. 4. Swelling index (%) of the developed inserts, depicted as mean ± SD (n = 3).

6.7. TGA

TGA analysis was conducted to evaluate the thermal behaviour of individual functional ingredients during and after their processing in HME. Considering that HME involves subjecting the polymer and drug to elevated temperatures, it is crucial to determine the stability of all materials at these processing temperatures. The TGA thermograms of castor oil, HPC, dexamethasone, and PEG 400, along with those of their physical mixture and optimized insert, are presented in **Fig. 5.** The results demonstrated that each component, including castor oil, HPC, dexamethasone, and PEG 400, exhibited sufficient stability at the HME processing temperature. Additionally, the TGA thermograms of both the physical mixture and the optimized insert indicated satisfactory stability, with no significant decomposition observed up to and above the processing temperature.

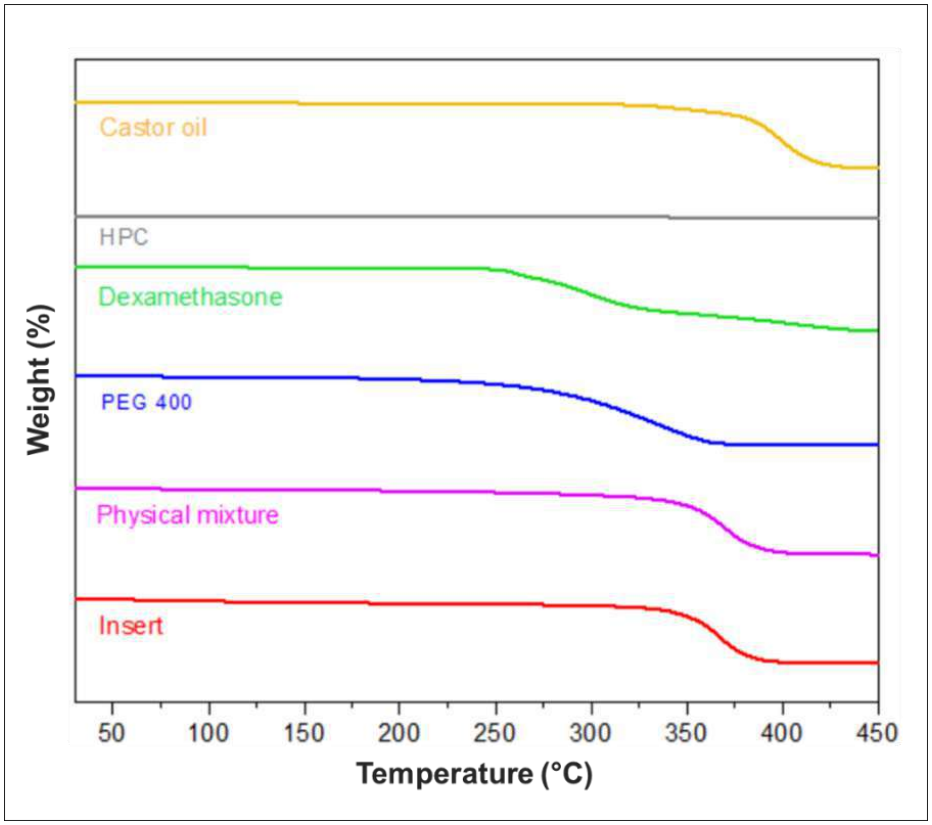

Fig. 5. TGA thermograms of castor oil; HPC; dexamethasone; PEG 400; physical mixture of castor oil, HPC, dexamethasone, PEG 400; and developed insert, respectively.

6.8. DSC

The DSC thermograms of dexamethasone, HPC, physical mixture of components of optimized insert and optimized insert are illustrated in **Fig. 6.** A characteristic endotherm of dexamethasone was observed at 255°C, whereas HPC showed no endotherm, aligning with the literature. Both the physical mixture and the optimized insert showed the absence of an endotherm indicating solubilization or amorphization of the drug within the polymeric insert.

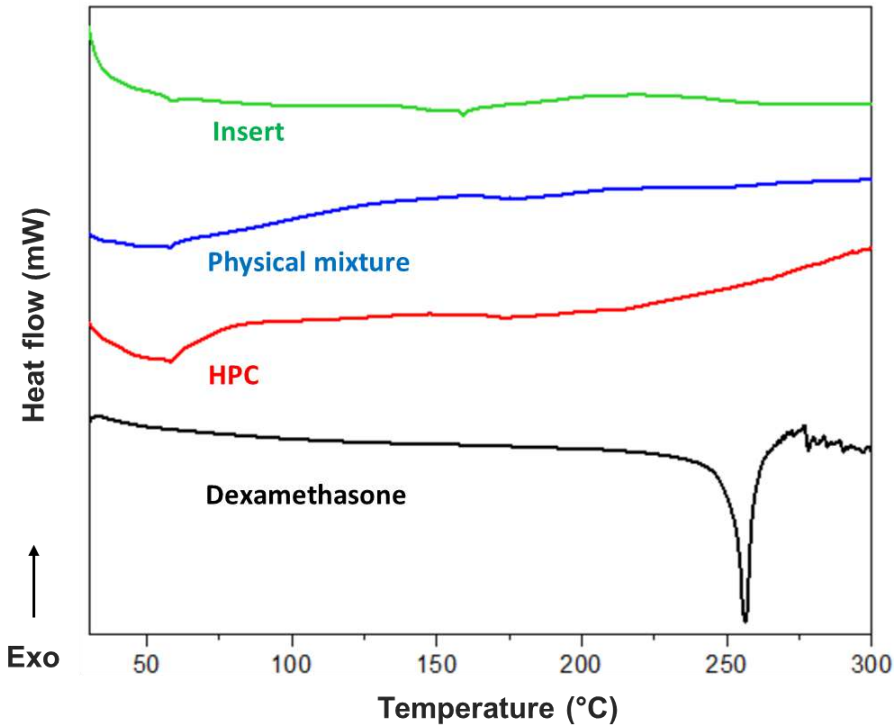

Fig. 6. DSC thermograms of dexamethasone; HPC; physical mixture of optimized insert and optimized insert, respectively.

6.9. XRD

The XRD diffractograms of dexamethasone, HPC, the physical mixture of the optimized formulation, and the optimized insert are shown in **Fig. 7**. The XRD pattern of the drug exhibited some intense and narrow diffraction peaks, representing the characteristic diffraction peaks of dexamethasone. On the other hand, HPC, the physical mixture, and the optimized insert showed the absence of sharp peaks, indicating the amorphous nature of the drug in the formulation.

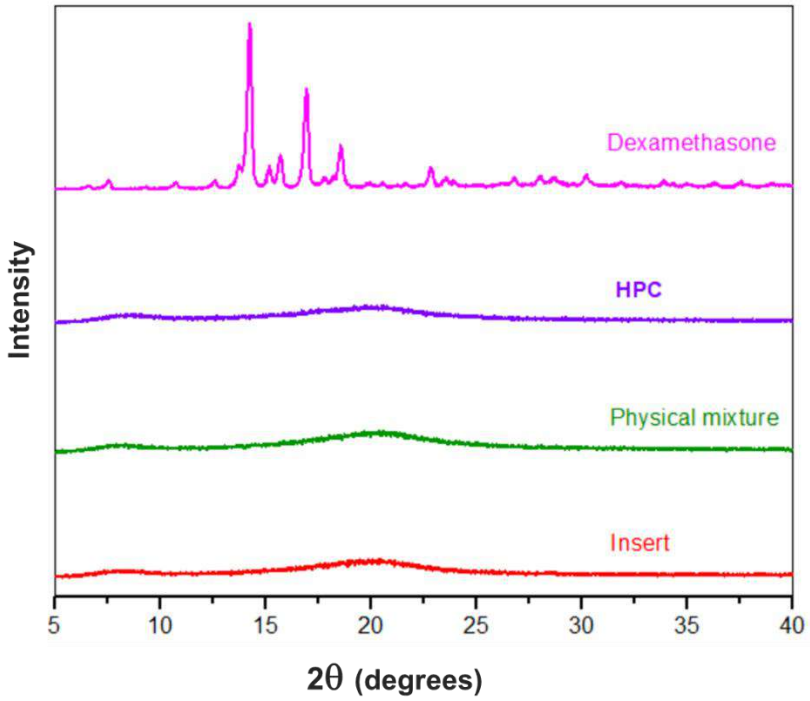

Fig. 7. XRD spectra of dexamethasone; HPC; physical mixture of optimized insert and optimized insert, respectively.

6.10. ATR-FTIR spectroscopy

The compatibility among the functional ingredients, along with potential interactions, was explored using ATR-FTIR spectroscopy [44]. In **Fig. 8**, the obtained FTIR-ATR spectra of castor oil, HPC, dexamethasone, PEG 400, as well as the physical mixture of the optimized insert and the optimized insert itself, are illustrated. Distinctive peaks corresponding to the standard characteristics of castor oil, HPC, dexamethasone, and PEG 400 were apparent in their respective spectra. Notably, for castor oil, the peak at 1733 cm^{-1} signifies C=O stretching, while the broader peak at 3492 cm^{-1} indicates O-H stretching [45]. Similarly, HPC exhibited a band around 3400 cm^{-1} attributed to the O-H group, with the band at 1058 cm^{-1} representing C-O stretching vibration [46]. Analysis of dexamethasone spectra revealed characteristic absorption bands at 3387 cm^{-1} due to O-H bond stretching, along with stretching vibrations at 1705, 1662, and 1620 cm^{-1} corresponding to -C=O and double bond framework conjugated to -C=O bonds [47][48]. In the case of PEG 400, the peak at 3445 cm^{-1} can be attributed to -OH stretching, and 2866 cm^{-1} to $-CH_2-$ stretching [49]. Furthermore, peaks at 1455 cm^{-1} and 1350 cm^{-1} are attributed to C-H bending [50]. The characteristic peaks of each component were found in the spectra of the physical mixture and insert suggesting an absence of incompatibility.

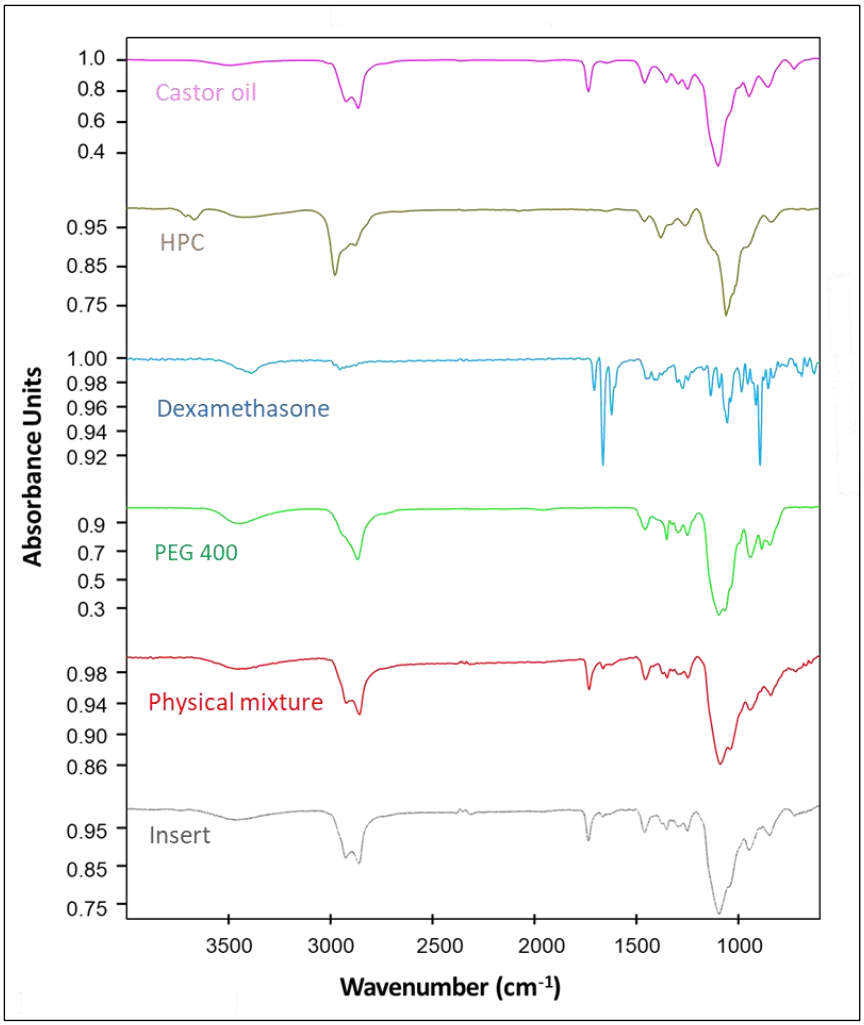

Fig. 8. ATR-FTIR spectra of castor oil; HPC; dexamethasone; PEG 400; physical mixture of optimized insert and optimized insert, respectively.

6.11. Optical microscopy, SEM and EDS

The morphology of the inserts was assessed employing an optical microscope. **Fig. 9(A-D)** illustrates the visual representations obtained by the microscope. The SEM analysis conducted in this study offered significant insights into the morphology of the drug, the physical mixture, and optimized inserts, as illustrated in **Fig. 10.** Inserts featuring sharp edges may cause inconvenience upon insertion, potentially leading to patient non-compliance or adverse reactions. Additionally, the smooth surface and absence of sharp edges on the inserts contribute to their biocompatibility, resulting in less inflammation. As evident from **Fig. 10**, the inserts exhibited smooth surfaces and edges, enhancing ease of administration. These visual representations clearly reveal the absence of any sharp edges or rough surface on the developed ocular inserts. It is important to emphasize that biocompatibility is not an intrinsic property of a material; rather, it hinges on the biological environment and the specific interactions

involving drug-polymer-tissue components [51]. Implants/inserts with smooth surfaces and devoid of sharp edges are generally more biocompatible and trigger less inflammation [52]. Therefore, prioritizing smoother implant/insert designs, while avoiding sharp corners that can lead to tissue damage during movement, becomes imperative to minimize local tissue damage and the development of chronic foreign body responses [53]. Particularly in the context of ocular inserts, maintaining a smooth surface and edges is of paramount importance. This is crucial to ensure patient acceptance and minimize potential issues. Overall, the SEM findings indicate that the optimized inserts possess advantageous morphological attributes conducive to both comfortable administration and effective drug delivery.

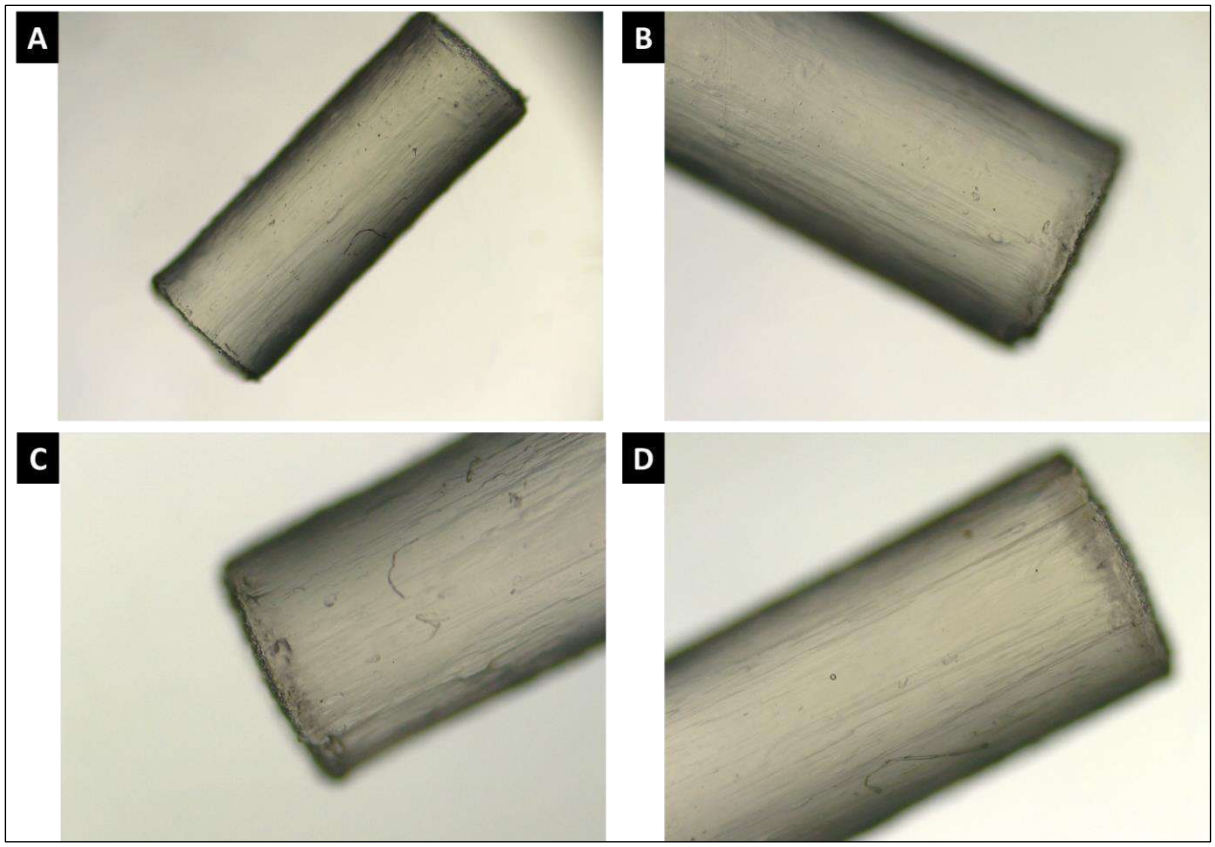

Fig 9. Optical microscopic images of the developed inserts **(A)** Entire insert (magnification: 2.5x) **(B), (C)** and **(D)** Surface and edges of inserts (magnification: 4x).

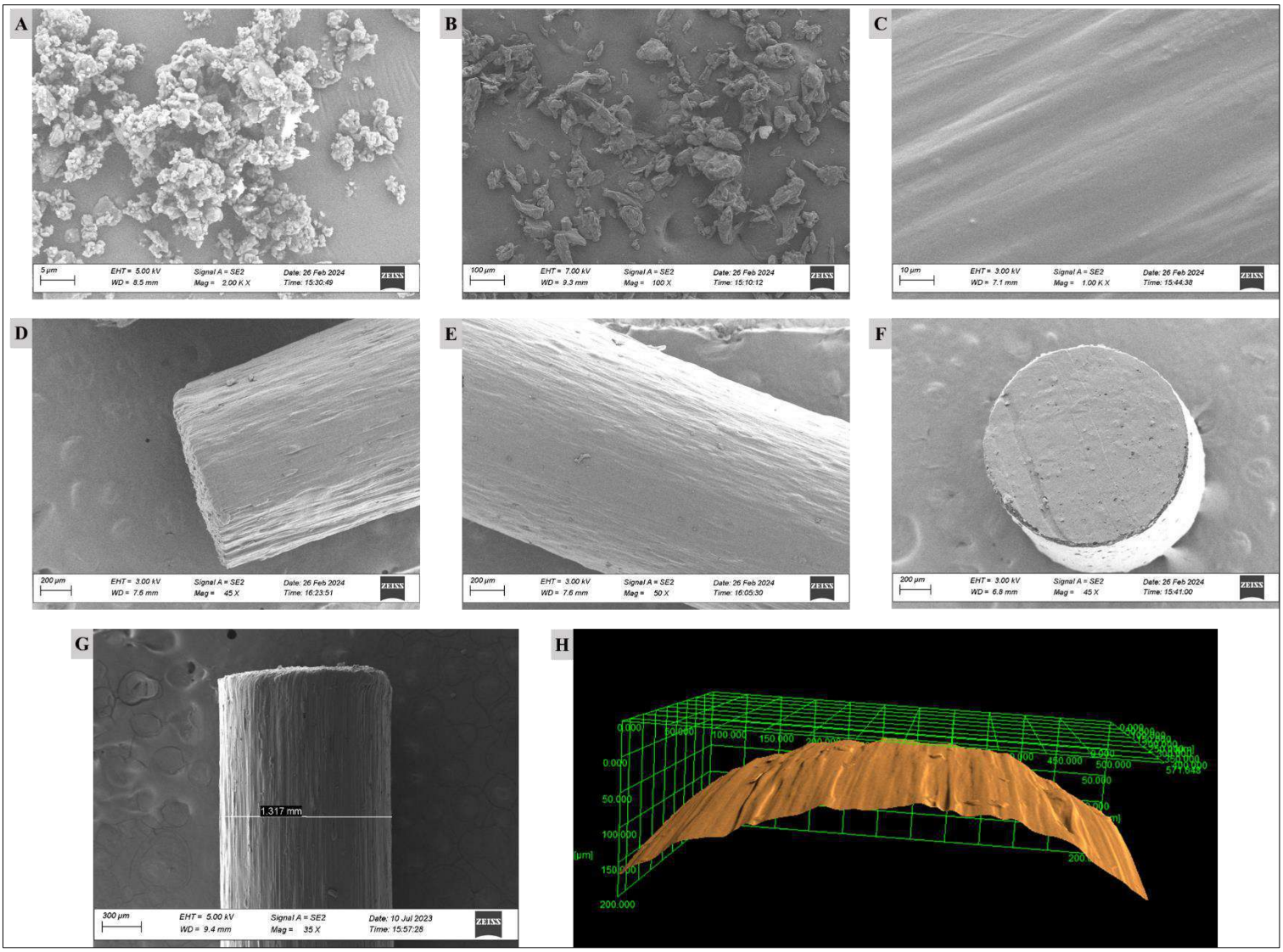

Fig. 10. SEM images of **(A)** Dexamethasone (Scale bar: 5 µm), **(B)** Physical mixture of castor oil, HPC, dexamethasone, PEG 400 (Scale bar: 100 µm), **(C)** Optimized insert (Scale bar: 10 µm), **(D-E)** Edge and surface of the optimized insert (Scale bar: 200 µm), **(F)** Cross section of the insert (Scale bar: 200 µm), **(G)** Edge (Scale bar: 300µm), **(H)** 3-D SEM image demonstrating the surface topography.

The presence of fluorine (F) atoms, identified through EDS analysis during SEM imaging of the optimized inserts, serves as a distinct indicator of uniform dexamethasone distribution within the polymeric carriers used for extrusion (**Fig. 11**). Since the other functional ingredients of the optimized inserts lack fluorine atoms in their structure, any fluorine detected can be attributed solely to dexamethasone. This highlights the efficiency of HME in achieving consistent mixing of ingredients, ensuring development of reliable drug delivery systems.

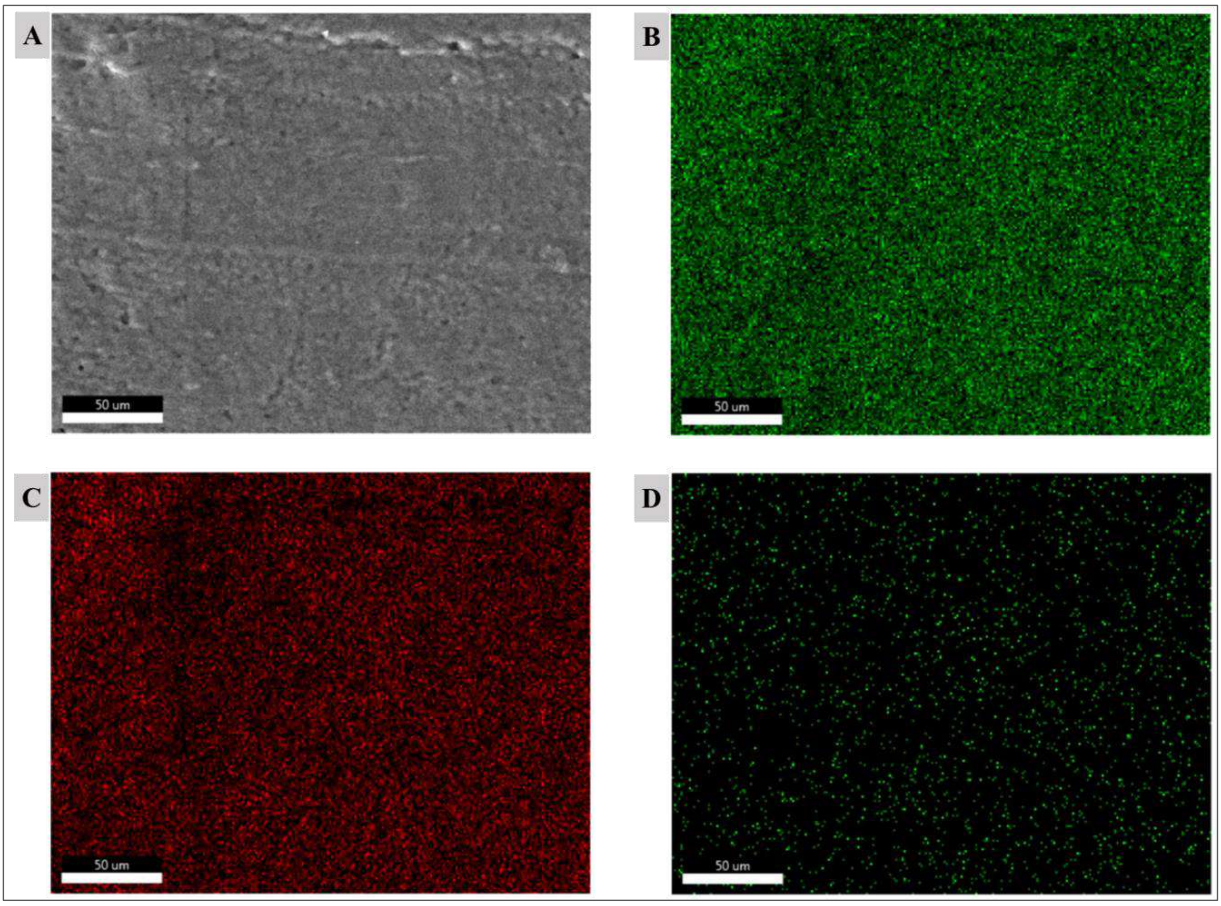

Fig. 11. EDS analysis of optimized ocular inserts depicting **(A)** SEM micrograph of the area analyzed, **(B)** Carbon – C, **(C)** Oxygen – O, **(D)** Fluorine – F.

6.12. *In vitro* release

The *in vitro* release study was conducted to evaluate the drug release behaviour of the optimized inserts. Results revealed that around 90.79 ± 1.48 % of the drug was released over a period of 15 hours, indicating sustained drug release characteristics. Notably, upon visual inspection, it was observed that the inserts began to hydrate upon exposure to the release media introduced into the glass beaker. **Fig. 12** depicts the *in vitro* release profile of the drug plotted against time.

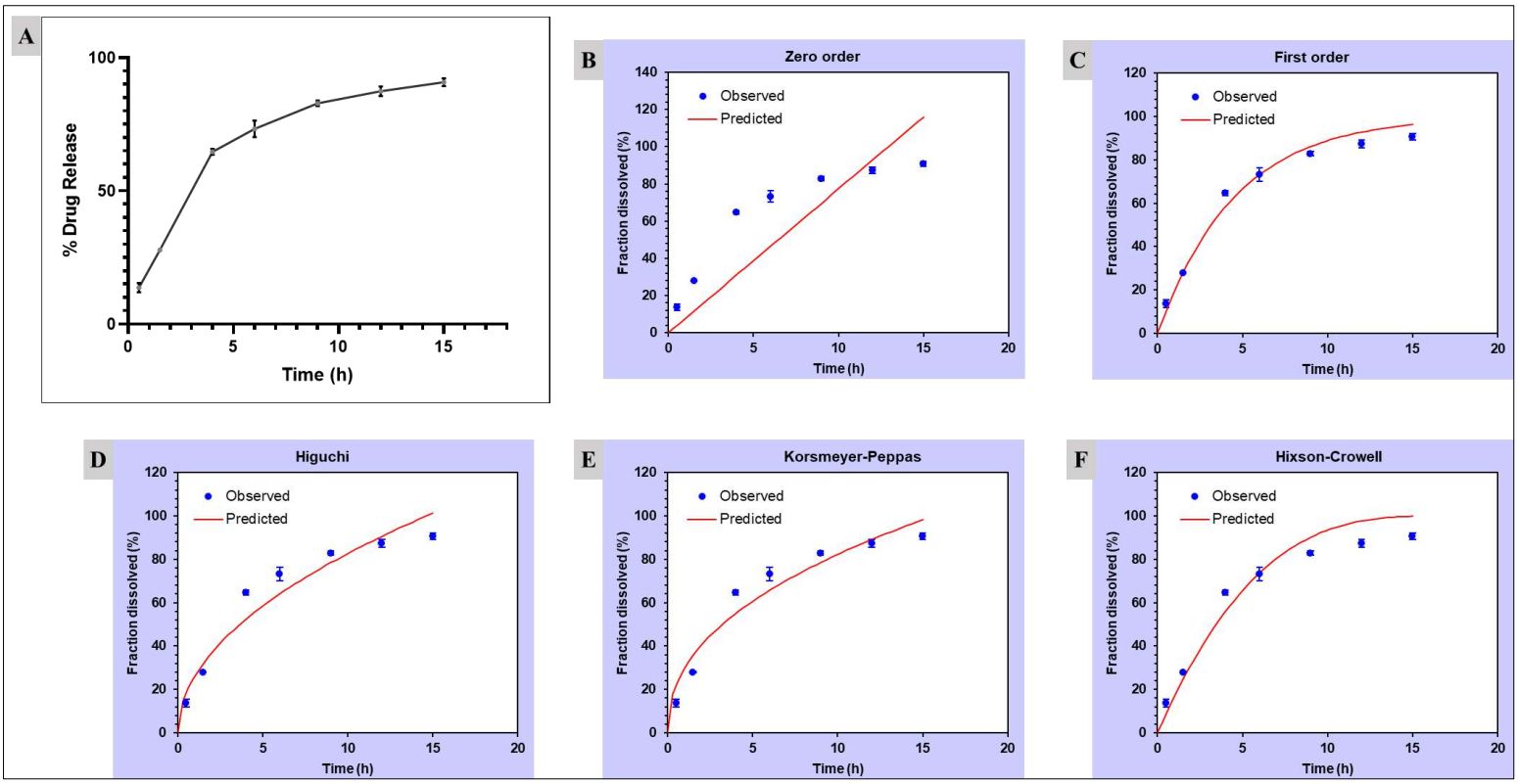

Fig. 12. *In vitro* drug release from the optimized inserts, depicted as mean ± SD (n = 3). The drug release values, both the ones that were observed and the ones that were predicted, are presented along with the model prediction using **(C)** Zero order, **(D)** First order, **(E)** Higuchi, **(F)** Korsmeyer-Peppas and **(G)** Hixson-Crowell.

The release mechanism of the developed inserts was investigated using DDSolver Software through regression analysis. Five conventional release models, namely Zero-order, First-order, Higuchi, Hixson-Crowell, and Korsmeyer-Peppas, were applied to fit the release profiles as shown in **Table 5**. In order to predict the drug release kinetics, the selection of the best model involves considering the highest R^2 value and the smallest AIC (Akaike Information Criterion) value. Additionally, a suitable model is determined when the MSC (modified reciprocal form of AIC) value is greater than 2 or 3. The mathematical model fitting revealed that the release profile from the inserts followed a first-order model. **Fig. 12B-F** displays multiple graphs, each representing distinct kinetic models.

Table 5 Statistical parameters of models to describe the release of drug from inserts.

Sr. no.	Model	Statistical paramter of model (mean ±SD)		
		R^2 Adj	AIC	MSC
1.	Zero Order	0.447 ± 0.018	58.203 ± 0.281	0.306 ±0.033

2.	**First Order**	**0.976 ± 0.005**	**36.008 ± 1.118**	**3.477 ± 0.212**
3.	Korsmeyer-Peppas	0.920 ± 0.010	45.351 ± 1.269	2.142 ± 0.127
4.	Higuchi	0.923 ± 0.007	44.382 ± 0.999	2.281 ± 0.090
5.	Hixson-Crowell	0.934 ± 0.010	43.237± 0.760	2.444 ± 0.161

6.13. *In vivo* irritation studies

The rabbits' eyes were inspected for any signs of irritation after 72 hours of instilling the ocular inserts. Throughout the entire evaluation period, the overall irritation scores for the irritancy test remained at 0 as evaluated for the cornea, iris, and conjunctiva. Findings revealed no apparent indications of redness or opacity in the cornea. Additionally, the iris and conjunctival blood vessels appeared normal, with no observed swelling in the eyelids. No adverse reactions were documented, and there was no notable distinction between the treated and untreated eyes. Consequently, the findings of the irritancy test demonstrate that the insert was non-toxic and does not cause irritation. However, the irritancy test does not clearly assess the level of comfort/discomfort of the insert. Furthermore, the inserts remained securely in the conjunctival sac of the eye and did not expel out, suggesting that the dimensions of the developed inserts were appropriate.

6.14. *In vivo* efficacy studies

6.14.1. Tear volume measurement

The treatment with benzalkonium chloride (0.1%) for 7 days showed a significant reduction in the wetted length in the Schirmer I eye test compared to the normal (baseline). These data suggest the induction of DES in the rabbit eye. Treatment with inserts following benzalkonium chloride administration showed a significant increase in the wetted length in the Schirmer I eye test compared to the disease control (untreated) (**Fig. 13**). These data indicate the beneficial effects of the inserts in treating DES.

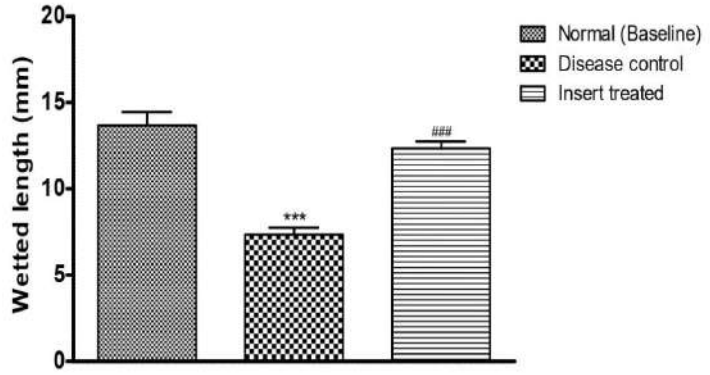

Fig. 13. Wetting length in Schirmer I eye test; depicted as mean ± SEM (n=6). ***P<0.001 vs normal baseline, $^{###}$P<0.001 vs Disease control.

7. Impact of the research in the advancement of knowledge or benefit to mankind

The integration of the CaliCut post-extrusion system with hot-melt extrusion (HME) marks a significant advancement in pharmaceutical dosage form manufacturing, enabling precise dimensional control and the creation of well-defined inserts. This combination has facilitated the efficient manufacturing of innovative ocular inserts for the management of Dry Eye Syndrome (DES), incorporating all necessary functional ingredients. Utilizing the Design of Experiments (DoE) approach has allowed for a comprehensive understanding of the impact of independent variables on the dependent variable, optimizing the formulation process.

Both in vitro and in vivo performances of the prepared ocular inserts were thoroughly examined, demonstrating their uniformity, consistency, and favorable physicochemical properties, including weight, dimensions, drug content, surface pH, moisture absorption, and swelling index. Thermal analysis confirmed the stability of individual ingredients and the optimized insert during processing, while spectroscopic analysis revealed compatibility among components. In vitro release studies exhibited sustained drug release characteristics, ensuring prolonged therapeutic effects. In vivo irritation studies demonstrated the biocompatibility and lack of irritancy associated with the ocular inserts, supporting their safe and well-tolerated use in ocular applications.

Notably, the study revealed an increase in tear volume following the application of optimized ocular inserts, thus supporting their in vivo efficacy and indicating their role in managing DES by effectively enhancing tear production. The developed ocular inserts facilitate convenient placement, enhancing patient compliance and potentially offering a longer-lasting effect. This advancement holds significant potential for improving the quality of life for individuals suffering from DES.

However, further development necessitates future studies, including in vivo pharmacokinetic and ocular biodistribution studies, to fully realize the potential of this innovative therapeutic approach. The strategic integration of CaliCut alongside HME and DoE methodologies has resulted in the effective development and assessment of ocular inserts, signifying advancements in pharmaceutical precision and productivity. This research not only advances the field of ocular drug delivery but also contributes to the broader scientific understanding of formulation optimization and manufacturing efficiency, ultimately benefiting mankind by providing a more effective and patient-friendly treatment for DES.

8. Literature references

[1] S. P. Phadatare, M. Momin, P. Nighojkar, S. Askarkar, and K. K. Singh, 'A Comprehensive Review on Dry Eye Disease: Diagnosis, Medical Management, Recent Developments, and Future Challenges', *Advances in Pharmaceutics*, vol. 2015, pp. 1–12, Jan. 2015, doi: 10.1155/2015/704946.

[2] J. Prinz, N. Maffulli, M. Fuest, P. Walter, A. Bell, and F. Migliorini, 'Efficacy of Topical Administration of Corticosteroids for the Management of Dry Eye Disease: Systematic Review and Meta-Analysis', *Life 2022, Vol. 12, Page 1932*, vol. 12, no. 11, p. 1932, Nov. 2022, doi: 10.3390/LIFE12111932.

[3] B. S. Lee, A. G. Kabat, J. Bacharach, P. Karpecki, and J. Luchs, 'Managing Dry Eye Disease and Facilitating Realistic Patient Expectations: A Review and Appraisal of Current Therapies', *Clin Ophthalmol*, vol. 14, p. 119, 2020, doi: 10.2147/OPTH.S228838.

[4] M. C. ristina Coroi, S. Bungau, and M. Tit, 'PRESERVATIVES FROM THE EYE DROPS AND THE OCULAR SURFACE', *Rom J Ophthalmol*, vol. 59, no. 1, p. 2, Jan. 2015.

[5] A. Kumari, P. K. Sharma, V. K. Garg, and G. Garg, 'Ocular inserts — Advancement in therapy of eye diseases', *J Adv Pharm Technol Res*, vol. 1, no. 3, p. 291, 2010, doi: 10.4103/0110-5558.72419.

[6] A. Alzahrani *et al.*, 'Formulation development and in Vitro–Ex vivo characterization of hot-melt extruded ciprofloxacin hydrochloride inserts for ocular applications: Part I', *Int J Pharm*, vol. 630, p. 122423, Jan. 2023, doi: 10.1016/J.IJPHARM.2022.122423.

[7] 'Thermo CaliCut '. Accessed: Aug. 11, 2023. [Online]. Available: https://assets.thermofisher.com/TFS-Assets/MSD/Technical-Notes/TN623-4005-CaliCut-post-extrusion-system.pdf

[8] D. Rana *et al.*, 'Precise Fabrication of Ocular Inserts Using an Innovative Laser-Driven CaliCut Technology: In Vitro and in Vivo Evaluation', *J Pharm Sci*, Dec. 2023, doi: 10.1016/J.XPHS.2023.12.015.

[9] C. Maïssa, M. Guillon, P. Simmons, and J. Vehige, 'Effect of castor oil emulsion eyedrops on tear film composition and stability', *Cont Lens Anterior Eye*, vol. 33, no. 2, pp. 76–82, Apr. 2010, doi: 10.1016/J.CLAE.2009.10.005.

[10] E. Goto *et al.*, 'Low-concentration homogenized castor oil eye drops for noninflamed obstructive meibomian gland dysfunction', *Ophthalmology*, vol. 109, no. 11, pp. 2030–2035, Nov. 2002, doi: 10.1016/S0161-6420(02)01262-9.

[11] E. C. Sandford, A. Muntz, and J. P. Craig, 'Therapeutic potential of castor oil in managing blepharitis, meibomian gland dysfunction and dry eye', *Clin Exp Optom*, vol. 104, no. 3, pp. 315–322, Apr. 2021, doi: 10.1111/CXO.13148.

[12] 'Artificial Tears: A Primer'. Accessed: Feb. 13, 2024. [Online]. Available: https://webeye.ophth.uiowa.edu/eyeforum/tutorials/artificial-tears.htm

[13] A. Kathuria, K. Shamloo, V. Jhanji, and A. Sharma, ‘Categorization of Marketed Artificial Tear Formulations Based on Their Ingredients: A Rational Approach for Their Use’, *J Clin Med*, vol. 10, no. 6, pp. 1–11, Mar. 2021, doi: 10.3390/JCM10061289.

[14] ‘SYSTANE ULTRA- polyethylene glycol 400 and propylene glycol solution/ drops’. Accessed: Feb. 13, 2024. [Online]. Available: https://fda.report/DailyMed/a5c1c194-3db5-4f18-9cd1-97f7f84c3cff

[15] S. Srinivasan and V. Manoj, ‘A decade of effective dry eye disease management with systane ultra (Polyethylene glycol/propylene glycol with hydroxypropyl guar) lubricant eye drops’, *Clinical Ophthalmology*, vol. 15, pp. 2421–2435, 2021, doi: 10.2147/OPTH.S294427.

[16] U. Benelli, ‘Systane® lubricant eye drops in the management of ocular dryness’, *Clinical Ophthalmology*, vol. 5, no. 1, pp. 783–790, 2011, doi: 10.2147/OPTH.S13773.

[17] ‘DailyMed - BLINK TEARS- polyethylene glycol 400 solution/ drops’. Accessed: Feb. 13, 2024. [Online]. Available: https://dailymed.nlm.nih.gov/dailymed/drugInfo.cfm?setid=10fcf407-6eaf-4730-9ed0-9b7715cf5701

[18] ‘LACRISERT- hydroxypropyl cellulose insert’. Accessed: Jul. 20, 2022. [Online]. Available: https://fda.report/DailyMed/cc7a6a52-0b77-4df7-8403-dd21c1334f6c

[19] I. Karnik *et al.*, ‘Formulation development and characterization of dual drug loaded hot-melt extruded inserts for better ocular therapeutic outcomes: Sulfacetamide/prednisolone’, *J Drug Deliv Sci Technol*, vol. 84, p. 104558, Jun. 2023, doi: 10.1016/J.JDDST.2023.104558.

[20] G. Loreti, A. Maroni, M. D. Del Curto, A. Melocchi, A. Gazzaniga, and L. Zema, ‘Evaluation of hot-melt extrusion technique in the preparation of HPC matrices for prolonged release’, *European Journal of Pharmaceutical Sciences*, vol. 52, no. 1, pp. 77–85, Feb. 2014, doi: 10.1016/J.EJPS.2013.10.014.

[21] G. Shadambikar *et al.*, ‘Novel Application of Hot Melt Extrusion Technology for Preparation and Evaluation of Valacyclovir Hydrochloride Ocular Inserts’, *AAPS PharmSciTech*, vol. 22, no. 1, Jan. 2021, doi: 10.1208/S12249-020-01916-5.

[22] Y. Wei and P. A. Asbell, ‘The Core Mechanism of Dry Eye Disease (DED) Is Inflammation’, *Eye Contact Lens*, vol. 40, no. 4, p. 248, 2014, doi: 10.1097/ICL.0000000000000042.

[23] X. Li, X. Jin, J. Wang, X. Li, and H. Zhang, ‘Dexamethasone attenuates dry eye-induced pyroptosis by regulating the KCNQ1OT1/miR-214 cascade’, *Steroids*, vol. 186, p. 109073, Oct. 2022, doi: 10.1016/J.STEROIDS.2022.109073.

[24] A. Jadhav, S. Salave, D. Rana, and D. Benival, ‘Development and In-vitro Evaluation of Dexamethasone Enriched Nanoemulsion for Ophthalmic Indication’, *Drug Deliv Lett*, vol. 13, no. 3, pp. 196–212, Mar. 2023, doi: 10.2174/2210303113666230309151048.

[25] S. Prodduturi, R. V. Manek, W. M. Kolling, S. P. Stodghill, and M. A. Repka, 'Water vapor sorption of hot-melt extruded hydroxypropyl cellulose films: Effect on physico-mechanical properties, release characteristics, and stability', *J Pharm Sci*, vol. 93, no. 12, pp. 3047–3056, Dec. 2004, doi: 10.1002/jps.20222.

[26] T. Fisher Scientific, 'PRODUCT SPECIFICATIONS Thermo Scientific CaliCut Post-extrusion System'.

[27] A. Alzahrani *et al.*, 'Design and optimization of ciprofloxacin hydrochloride biodegradable 3D printed ocular inserts: Full factorial design and in-vitro and ex-vivo evaluations: Part II', *Int J Pharm*, vol. 631, p. 122533, Jan. 2023, doi: 10.1016/J.IJPHARM.2022.122533.

[28] R. Thakkar, N. Komanduri, N. Dudhipala, S. Tripathi, M. A. Repka, and S. Majumdar, 'Development and optimization of hot-melt extruded moxifloxacin hydrochloride inserts, for ocular applications, using the design of experiments', *Int J Pharm*, vol. 603, Jun. 2021, doi: 10.1016/J.IJPHARM.2021.120676.

[29] A. M. Alambiaga-Caravaca *et al.*, 'Development, characterization, and ex vivo evaluation of an insert for the ocular administration of progesterone', *Int J Pharm*, vol. 606, Sep. 2021, doi: 10.1016/J.IJPHARM.2021.120921.

[30] K. S. Prayag, A. T. Paul, S. K. Ghorui, and A. B. Jindal, 'Preparation and Evaluation of Quinapyramine Sulphate-Docusate Sodium Ionic Complex Loaded Lipidic Nanoparticles and Its Scale Up Using Geometric Similarity Principle', *J Pharm Sci*, vol. 110, no. 5, pp. 2241–2249, May 2021, doi: 10.1016/J.XPHS.2021.01.033.

[31] P. V. Dangre, R. D. Phad, S. J. Surana, and S. S. Chalikwar, 'Quality by design (QbD) assisted fabrication of fast dissolving buccal film for clonidine hydrochloride: Exploring the quality attributes', *Advances in Polymer Technology*, vol. 2019, 2019, doi: 10.1155/2019/3682402.

[32] S. Tambe *et al.*, 'MeltSerts technology (brinzolamide ocular inserts via hot-melt extrusion): QbD-steered development, molecular dynamics, in vitro, ex vivo and in vivo studies', *Int J Pharm*, vol. 648, p. 123579, Dec. 2023, doi: 10.1016/J.IJPHARM.2023.123579.

[33] S. Taghe, S. Mirzaeei, and A. Ahmadi, 'Preparation and Evaluation of Nanofibrous and Film-Structured Ciprofloxacin Hydrochloride Inserts for Sustained Ocular Delivery: Pharmacokinetic Study in Rabbit's Eye', *Life 2023, Vol. 13, Page 913*, vol. 13, no. 4, p. 913, Mar. 2023, doi: 10.3390/LIFE13040913.

[34] D. Rana, S. Salave, S. Jain, R. Shah, and D. Benival, 'Systematic Development and Optimization of Teriparatide-Loaded Nanoliposomes Employing Quality by Design Approach for Osteoporosis', *Journal of Pharmaceutical Innovation*, pp. 1–15, Jun. 2022, doi: 10.1007/S12247-022-09663-9/METRICS.

[35] 'Section 4 Health effects OECD/OCDE 405 OECD GUIDELINE FOR THE TESTING OF CHEMICALS', 2021, Accessed: Feb. 08, 2023. [Online]. Available: http://www.oecd.org/termsandconditions/.

[36] O. E. Muz *et al.*, ‘A Novel Integrated Active Herbal Formulation Ameliorates Dry Eye Syndrome by Inhibiting Inflammation and Oxidative Stress and Enhancing Glycosylated Phosphoproteins in Rats’, *Pharmaceuticals (Basel)*, vol. 13, no. 10, pp. 1–18, Oct. 2020, doi: 10.3390/PH13100295.

[37] C. Li *et al.*, ‘Research on the stability of a rabbit dry eye model induced by topical application of the preservative benzalkonium chloride’, *PLoS One*, vol. 7, no. 3, Mar. 2012, doi: 10.1371/JOURNAL.PONE.0033688.

[38] D. Jiang, J. Hu, and X. Liu, ‘Topical administration of Esculetin as a potential therapy for experimental dry eye syndrome’, *Eye 2017 31:12*, vol. 31, no. 12, pp. 1724–1732, Jun. 2017, doi: 10.1038/eye.2017.117.

[39] S. Salave *et al.*, ‘Recent Progress in Hot Melt Extrusion Technology in Pharmaceutical Dosage Form Design’, *Recent Adv Drug Deliv Formul*, vol. 16, no. 3, pp. 170–191, Sep. 2022, doi: 10.2174/2667387816666220819124605.

[40] S. K. Vemula, B. Daravath, and M. Repka, ‘Quality by design (QbD) approach to develop fast-dissolving tablets using melt-dispersion paired with surface-adsorption method: formulation and pharmacokinetics of flurbiprofen melt-dispersion granules’, *Drug Deliv Transl Res*, vol. 13, no. 12, pp. 3204–3222, Dec. 2023, doi: 10.1007/S13346-023-01382-Z/METRICS.

[41] ‘Stat-Ease » v12 » Hints and FAQs » Screen Tips » Contour Plot’. Accessed: Mar. 12, 2024. [Online]. Available: https://www.statease.com/docs/v12/screen-tips/analysis-node/contour-plot/

[42] D. Rana, S. Salave, S. Jain, R. Shah, and D. Benival, ‘Systematic Development and Optimization of Teriparatide-Loaded Nanoliposomes Employing Quality by Design Approach for Osteoporosis’, *J Pharm Innov*, pp. 1–15, Jun. 2022, doi: 10.1007/S12247-022-09663-9/METRICS.

[43] ‘⟨771⟩ Ophthalmic Products—Quality Tests’. Accessed: Mar. 22, 2024. [Online]. Available: https://doi.usp.org/USPNF/USPNF_M99560_04_01.html

[44] J. Viljoen *et al.*, ‘Formulation Development of Solid Self-Nanoemulsifying Drug Delivery Systems of Quetiapine Fumarate via Hot-Melt Extrusion Technology: Optimization Using Central Composite Design’, *Pharmaceutics 2024, Vol. 16, Page 324*, vol. 16, no. 3, p. 324, Feb. 2024, doi: 10.3390/PHARMACEUTICS16030324.

[45] H. Jahangirian *et al.*, ‘Enzymatic Synthesis of Ricinoleyl Hydroxamic Acid Based on Commercial Castor Oil, Cytotoxicity Properties and Application as a New Anticancer Agent’, *Int J Nanomedicine*, vol. 15, p. 2935, 2020, doi: 10.2147/IJN.S223796.

[46] N. D. Alharbi and O. W. Guirguis, ‘Macrostructure and optical studies of hydroxypropyl cellulose in pure and Nano-composites forms’, *Results Phys*, vol. 15, p. 102637, Dec. 2019, doi: 10.1016/J.RINP.2019.102637.

[47] C. Wang, H. Hou, K. Nan, M. J. Sailor, W. R. Freeman, and L. Cheng, ‘Intravitreal controlled release of dexamethasone from engineered microparticles of porous silicon dioxide’, *Exp Eye Res*, vol. 129, pp. 74–82, Dec. 2014, doi: 10.1016/J.EXER.2014.11.002.

[48] J. Long, A. V. Nand, C. Bunt, and A. Seyfoddin, ‘Controlled release of dexamethasone from poly(vinyl alcohol) hydrogel’, *Pharm Dev Technol*, vol. 24, no. 7, pp. 839–848, Aug. 2019, doi: 10.1080/10837450.2019.1602632.

[49] X. Bai *et al.*, ‘Preparation and evaluation of amine terminated polyether shale inhibitor for water-based drilling fluid’, *SN Appl Sci*, vol. 1, no. 1, pp. 1–9, Jan. 2019, doi: 10.1007/S42452-018-0112-X/TABLES/5.

[50] M. T. Caccamo and S. Magazù, ‘Multiscale Spectral Analysis on Lysozyme Aqueous Solutions in the Presence of PolyEthyleneGlycol’, *Molecules 2022, Vol. 27, Page 8760*, vol. 27, no. 24, p. 8760, Dec. 2022, doi: 10.3390/MOLECULES27248760.

[51] H. K. Makadia and S. J. Siegel, ‘Poly Lactic-co-Glycolic Acid (PLGA) as Biodegradable Controlled Drug Delivery Carrier’, *Polymers*, vol. 3, no. 3, p. 1377, Sep. 2011, doi: 10.3390/POLYM3031377.

[52] O. Veiseh and A. J. Vegas, ‘Domesticating the foreign body response: Recent advances and applications’, *Advanced Drug Delivery Reviews*, vol. 144, pp. 148–161, Apr. 2019, doi: 10.1016/J.ADDR.2019.08.010.

[53] A. Carnicer-Lombarte, S. T. Chen, G. G. Malliaras, and D. G. Barone, ‘Foreign Body Reaction to Implanted Biomaterials and Its Impact in Nerve Neuroprosthetics’, *Frontiers in Bioengineering and Biotechnology*, vol. 9, p. 622524, Apr. 2021, doi: 10.3389/FBIOE.2021.622524/BIBTEX.

Dhwani Rana

PhD Scholar

Department of Pharmaceutics

NIPER – Ahmedabad

Email Id: dhwani.rana@niperahm.res.in